

# Stability and Lifetime of Quadruply Hydrogen Bonded 2-Ureido-4[1H]-pyrimidinone Dimers

Serge H. M. Söntjens, Rint P. Sijbesma,\* Marcel H. P. van Genderen, and E. W. Meijer

Contribution from the Laboratory of Macromolecular and Organic Chemistry, Eindhoven University of Technology, P.O. Box 513, 5600 MB Eindhoven, The Netherlands

Received February 4, 2000

**Abstract:** 2-Ureido-4[1H]-pyrimidinones are known to dimerize via a strong quadruple hydrogen bond array. A detailed study of the dimerization constant and lifetime of the dimer is presented here. Excimer fluorescence of pyrene-labeled 2-ureido-4[1H]-pyrimidinone **1b** was used to determine a dimerization constant  $K_{\text{dim}}$  of  $6 \times 10^7 \text{ M}^{-1}$  in  $\text{CHCl}_3$ ,  $1 \times 10^7 \text{ M}^{-1}$  in chloroform saturated with water, and  $6 \times 10^8 \text{ M}^{-1}$  in toluene (all at 298 K). Under these conditions, the preexchange lifetime of the similar dimers of both **1d** and **1e** is 170 ms in  $\text{CDCl}_3$ , 80 ms in wet  $\text{CDCl}_3$ , and 1.7 s in toluene- $d_8$ , as determined by dynamic NMR spectroscopy. Association rate constants were calculated from the  $K_{\text{dim}}$  values and the preexchange lifetimes. The resulting values are significantly lower than the diffusion-controlled association rate constants calculated using the Stokes–Einstein and the Debye equations. This difference is ascribed to a tautomeric equilibrium of the monomer between the dimerizing 4[1H]-pyrimidinone and nondimerizing 6[1H]-pyrimidinone tautomers, which is unfavorable for dimerization.

## Introduction

One of the challenges in supramolecular chemistry is the construction of molecules that associate in a strong, directional, and selective way.<sup>1</sup> The successful assembly of large and stable supramolecular structures relies on the availability of such building blocks.<sup>2</sup> Often multiple hydrogen bonds constitute the required interactions between these building blocks.<sup>3</sup> Arrays with three hydrogen bonds are well-known from the base pairing between purines and pyrimidines in DNA, and numerous synthetic triply hydrogen bonded molecules are known with other donor (D) and acceptor (A) arrays.<sup>3</sup> The weakest association is observed between DAD and ADA arrays, as in the adenine–thymine dimer, with dimerization constants in the range of  $10^2$  to  $10^3 \text{ M}^{-1}$  in chloroform.<sup>3</sup> The DDA•AAD combination, as in the guanine–cytosine dimer, is also often used and has an approximate dimerization constant of  $10^4$  to  $10^5 \text{ M}^{-1}$  in chloroform.<sup>4,5</sup> Due to favorable secondary interactions,<sup>6</sup> the latter value is 2 to 3 orders of magnitude higher than that found for DAD•ADA dimers. More exotic and synthetically less accessible is the combination of AAA and DDD arrays, as pioneered by Zimmerman et al.,<sup>7–12</sup> with association constants exceeding  $10^5 \text{ M}^{-1}$ .

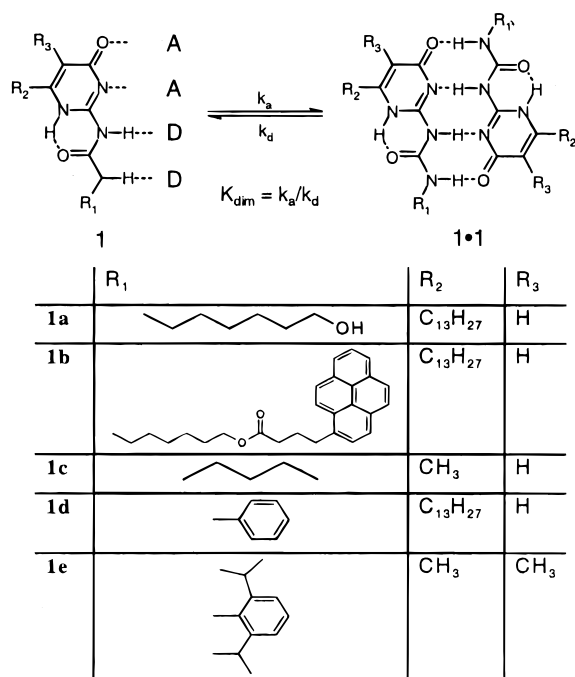
Quadruple hydrogen bond arrays have been predicted to be much stronger than triple hydrogen bond arrays.<sup>13</sup> An additional advantage is that with four hydrogen bonds, the construction of self-complementary molecules becomes possible, which simplifies the synthesis to just one molecule and avoids problems of exact stoichiometry of heterodimers. Recently, we have reported the strong dimerization of 2-ureido-4[1H]-pyrimidinone derivatives **1**, which feature a DDAA array of hydrogen bonding sites. The synthetically easily accessible self-complementary molecules are planarized by an intramolecular hydrogen bond and form strong dimers via quadruple hydrogen bonds.<sup>14</sup> High dimerization constants make these molecules very interesting building blocks for supramolecular chemistry, but they lead to great difficulty in measuring the dimerization constant accurately. A further complicating factor in the study of 2-ureido-4[1H]-pyrimidinone dimerization is the presence of different tautomeric forms of both the monomeric and the dimeric species.<sup>14</sup>

The strong association makes **1** particularly interesting for the formation of supramolecular polymers from molecules containing two 2-ureido-4[1H]-pyrimidinone groups connected by a spacer, as was recently reported by our group.<sup>15,16</sup> We have studied the bulk and solution properties of these supramolecular polymers using (dynamic) rheology and dielectric spectroscopy.

(1) Lehn, J.-M. *Supramolecular Chemistry*; VCH: Weinheim, 1995.  
(2) Sijbesma, R. P.; Meijer, E. W. *Curr. Opin. Colloid Interface Sci.* **1999**, *4*, 24–32.  
(3) Zimmerman, S. C.; Corbin, P. S. *Struct. Bonding* **2000**, *96*, 63–94.  
(4) Kelly, T. R.; Zhao, C.; Bridges, G. J. *J. Am. Chem. Soc.* **1989**, *111*, 3744.  
(5) Kyogoku, Y.; Lord, R. C.; Rich, A. *Biochim. Biophys. Acta* **1969**, *179*, 10.  
(6) Jorgensen, W. L.; Pranata, J. *J. Am. Chem. Soc.* **1990**, *112*, 2008–2010.  
(7) Murray, T. J.; Zimmerman, S. C. *J. Am. Chem. Soc.* **1992**, *114*, 4010–4011.  
(8) Fenlon, E. E.; Murray, T. J.; Baloga, M. H.; Zimmerman, S. C. *J. Org. Chem.* **1993**, *58*, 6625–6628.  
(9) Zimmerman, S. C.; Murray, T. J. *Philos. Trans. R. Soc. London, Ser. A* **1993**, *345*, 49–56.

(10) Zimmerman, S. C.; Murray, T. J. *Tetrahedron Lett.* **1994**, *35*, 4077–4080.  
(11) Murray, T. J.; Zimmerman, S. C.; Kolotuchin, S. V. *Tetrahedron* **1995**, *51*, 635–648.  
(12) Murray, T. J.; Zimmerman, S. C. *Tetrahedron Lett.* **1995**, *36*, 7627–7630.  
(13) Sartorius, J.; Schneider, H.-J. *Chem. Eur. J.* **1996**, *2*, 1446–1452.  
(14) Beijer, F. H.; Sijbesma, R. P.; Kooijman, H.; Spek, A. L.; Meijer, E. W. *J. Am. Chem. Soc.* **1998**, *120*, 6761–6769.  
(15) Sijbesma, R. P.; Beijer, F. H.; Brunsveld, L.; Folmer, B. J. B.; Hirschberg, J. H. K. K.; Lange, R. F. M.; Lowe, J. K. L.; Meijer, E. W. *Science* **1997**, *278*, 1601–1604.  
(16) Folmer, B. J. B.; Sijbesma, R. P.; Kooijman, H.; Spek, A. L.; Meijer, E. W. *J. Am. Chem. Soc.* **1999**, *121*, 9001–9007.

Scheme 1



copy.<sup>15,17</sup> These properties are directly influenced by the thermodynamic and kinetic parameters of the dimerization process.<sup>18–20</sup> It is, therefore, of great importance to gain detailed insight into the lifetime of the dimer and the dimerization constant both in solution and in bulk.

It proved impossible to determine the dimerization constant of **1** from NMR dilution experiments,<sup>21</sup> because no change in the NMR spectra was observed, even at concentrations near the detection limit using a high-field machine (up to 750 MHz). The dimerization constant is estimated as exceeding  $10^6 \text{ M}^{-1}$  in chloroform for the 2-ureido-4[1H]-pyrimidinones, including the occurrence of tautomers. A similar molecule (**2**) reported by Zimmerman,<sup>3,22</sup> lacking tautomers that interfere with hydrogen bonding, was reported to have a dimerization constant exceeding  $3 \times 10^7 \text{ M}$ .

There are two solutions to the detection limit problem presented above: a technique can be used with a detection limit significantly below  $10^{-6} \text{ M}$ , or an indirect method to detect the dissociation/association process may be employed. We present here a combination of techniques to obtain information on the solution dynamics of the dimerization process, which may be applied to very strongly binding complexes in general. Excimer fluorescence of pyrene-labeled **1b** was used to determine the equilibrium dimerization constant  $K_{\text{dim}}$  of two 2-ureido-4[1H]-pyrimidinones in different solvents. Pyrene is well-known to form excimer species in solution,<sup>23–25</sup> showing an emission band

that is well separated from the monomer emission band. This phenomenon has been used previously to determine association constants of pyrene-labeled compounds in solution.<sup>26–28</sup> Additionally we have used dynamic NMR studies (EXSY<sup>29–32</sup> and DPGSE<sup>33–38</sup>) to establish the preexchange lifetime of the dimers. Finally, we have compared NMR and fluorescence data and propose the presence of weakly dimerizing and nondimerizing tautomers of monomeric 2-ureido-4[1H]-pyrimidinone in solution to rationalize the data.

## Experimental Section

**General Methods.** Unless stated otherwise, all reagents and chemicals were obtained from commercial sources and used without further purification. Dry dichloromethane was distilled from  $\text{P}_2\text{O}_5$  before use. Deuterated chloroform was dried and de-acidified over activated alumina (type I) and stored on 4 Å molsieves. Wet deuterated chloroform was allowed to equilibrate under a water layer for 2 weeks until used. All routine  $^1\text{H}$  and  $^{13}\text{C}$  NMR measurements were recorded on a Bruker AM 400 or a Varian Mercury Vx 400 instrument unless indicated otherwise. All chemical shifts ( $\delta$ ) are reported in ppm downfield of TMS. Elemental analyses were performed on a Perkin-Elmer 2400 Series CHNS/O analyzer. Melting points were determined on a Jenaval polarization microscope with a Linkam THMS 600 hotstage, and are uncorrected.

Fluorescence measurements were performed on a Perkin-Elmer LS50B luminescence spectrometer with a thermostated cell. The chloroform used for fluorescence spectroscopy was of analytical grade and was filtered through a  $1 \mu\text{m}$  filter before use. The toluene for fluorescence spectroscopy was of analytical grade and was used as received. The chloroform saturated with water for fluorescence was stored under a water layer for 2 weeks to equilibrate. The amount of water in saturated chloroform is approximately 55 mM, estimated from NMR measurements with water-saturated  $\text{CDCl}_3$  (calibrated on the residual  $\text{CHCl}_3$  peak). The fluorescence cells used were thoroughly cleaned with hydrogen peroxide/concentrated sulfuric acid mixtures, water, acetone, and dichloromethane before use. The cells were cleaned repeatedly until a clear baseline without residual pyrene emission was obtained. Emission intensities  $I$  were integrated from 500 to 600 nm and the resulting data were fitted using a nonlinear curve fit protocol to  $I = \{C_1/8K_{\text{dim}}\}\{1 + 4K_{\text{dim}}[\text{Py}] - (1 + 8K_{\text{dim}}[\text{Py}])^{1/2}\}$ . This equation is obtained by assuming that the emission intensity  $I$  is proportional to  $[\text{Py}_{\text{dim}}]$ , which concentration is extracted from the equilibrium equation  $K_{\text{dim}} = [\text{Py}_{\text{dim}}]/[\text{Py}_{\text{mono}}]^2$  and the mass balance equation  $[\text{Py}] = 2[\text{Py}_{\text{dim}}] + [\text{Py}_{\text{mono}}]$ . In these equations  $[\text{Py}]$ ,  $[\text{Py}_{\text{mono}}]$ , and  $[\text{Py}_{\text{dim}}]$  are the total concentration and the concentration of monomeric and of dimeric pyrene labeled 2-ureido-4[1H]-pyrimidinone, respectively.

Mixed solutions of **1d** and **1e** used in exchange NMR were 10 mM for each component. Concentration-dependent EXSY exchange NMR

(17) Folmer, B. J. B.; Sijbesma, R. P.; Meijer, E. W. *Polym. Prepr.* **1999**, 80, 20–21.

(18) Leibler, L.; Rubinstein, M.; Colby, R. H. *Macromolecules* **1991**, 24, 4701–4707.

(19) Cates, M. E. *Macromolecules* **1987**, 20, 2289–2296.

(20) Cates, M. E. *J. Phys. Chem.* **1990**, 94, 371–375.

(21) Beijer, F. H. *Cooperative Multiple Hydrogen Bonding in Supramolecular Chemistry*; Thesis, Eindhoven University of Technology: Eindhoven, 1998; p 175.

(22) Corbin, P. S.; Zimmerman, S. C. *J. Am. Chem. Soc.* **1998**, 120, 9710–9711.

(23) Förster, T.; Kasper, K. Z. *Electrochem.* **1955**, 59, 976–980.

(24) Förster, T. *Angew. Chem.* **1969**, 81, 364–374.

(25) Birks, J. B.; Dyson, D. J.; Munro, I. H. *Proc. R. Soc. London, Ser. A* **1963**, 275, 575–588.

(26) Ikkai, T.; Kondo, H. *J. Biochem. Biophys. Methods* **1996**, 33, 55–58.

(27) García-Echeverría, C. *J. Am. Chem. Soc.* **1994**, 116, 6031–6032.

(28) Pistolis, G.; Paleos, C. M.; Malliaris, A. *J. Phys. Chem.* **1995**, 99, 8896–8901.

(29) Mogck, O.; Pons, M.; Böhmer, V.; Vogt, W. *J. Am. Chem. Soc.* **1997**, 119, 5706–5712.

(30) Dwyer, T. J.; Norman, J. E.; Jasien, P. G. *J. Chem. Educ.* **1998**, 75, 1635–1640.

(31) Perrin, C. L.; Dwyer, T. J. *Chem. Rev.* **1990**, 90, 935–967.

(32) Jeener, J.; Meier, B. H.; Bachmann, P.; Ernst, R. R. *J. Chem. Phys.* **1979**, 71, 4546–4553.

(33) Mariappan, S. V. S.; Rabenstein, D. L. *J. Magn. Reson.* **1992**, 100, 183–188.

(34) Dahlquist, F. W.; Longmuir, K. J.; Du Vernet, R. B. *J. Magn. Reson.* **1975**, 17, 406–410.

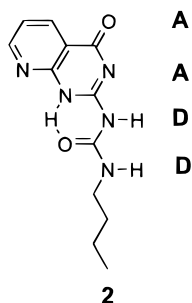
(35) McConnell, H. M. *J. Chem. Phys.* **1958**, 28, 430–431.

(36) Stonehouse, J.; Adell, P.; Keeler, J.; Shaka, A. J. *J. Am. Chem. Soc.* **1994**, 116, 6037–6038.

(37) Stott, K.; Stonehouse, J.; Keeler, J.; Hwang, T. L.; Shaka, A. J. *J. Am. Chem. Soc.* **1995**, 117, 4199–4200.

(38) Stott, K.; Keeler, J.; Van, Q. N.; Shaka, A. J. *J. Magn. Reson.* **1997**, 125, 302–324.

## Scheme 2



measurements were performed on a Bruker AM 400 spectrometer with a 5 mm QNP probe at 303 K. Temperature-dependent EXSY exchange NMR measurements and all DPFGE measurements were performed on a Bruker AVANCE DRX 600 spectrometer with a 5 mm TXI probe. For the DPFGE the Bruker pulse sequence selnpgp.3 was used with a ReBurp selective refocusing pulse, which was calibrated manually for optimal performance. Both homodimer and heterodimer peaks were selectively refocused and yielded the same value for  $k_d$ , within the error of the measurement. For measurements in  $\text{CDCl}_3$ , the methyl peak was used, and for measurement in octadeuteriotoluene, the alkylidene proton signal was used because of interference of the solvent signal with the methyl peaks. The EXSY data were evaluated using the response function  $\phi = \ln(r + 1/r - 1)$  where  $r = (I_{11} + I_{22})/(I_{12} + I_{21})$ , the ratio of diagonal- and cross-peak intensities.<sup>30,31</sup> These data were fitted using a linear least-squares fit to the kinetic equation  $\phi = k_{\text{ex}}t_{\text{mix}} \cdot T_1$  relaxation times in the DPFGE experiments were determined according to Dahlquist.<sup>34</sup> The DPFGE intensities were fitted, with a nonlinear algorithm, to the response functions<sup>33</sup>  $A = \{(1 + \alpha)A_0/(k_{\text{AX}} + k_{\text{XA}}) - \{k_{\text{XA}} \exp(-Rt) + k_{\text{AX}} \exp(-(R + k_{\text{AX}} + k_{\text{XA}})t)\}$  and  $X = \{(1 + \alpha)A_0/(k_{\text{AX}} + k_{\text{XA}})\}k_{\text{AX}}\{\exp(-Rt) - \exp(-(R + k_{\text{AX}} + k_{\text{XA}})t)\}$ , with A being the refocused peak (O, homodimer) and X being the dispersed peak (□, heterodimer),  $\alpha$  the inversion efficiency,  $A_0$  the equilibrium magnetization, and  $R = 1/T_1$ . The toluene data were fitted to the functions A and X simultaneously using Matlab; a  $r^2$  value could not be determined.

**Synthesis.** The syntheses of the ureidopyrimidinone molecules depicted in Scheme 1 are outlined below. 6-Isocyanatohexanol was prepared according to a procedure described by Versteegen<sup>39</sup> and Peerlings.<sup>40</sup> 6-Tridecylisocytosine was also synthesized according to literature procedures,<sup>14</sup> 5,6-dimethylisocytosine, *n*-butyl-1-ureido-4[1H]-pyrimidinone (**1c**), and 2-phenylureido-4[1H]-pyrimidinone (**1d**) were synthesized previously.<sup>14</sup>

**2-(6-Hydroxyhexylureido)-6-tridecyl-4[1H]-pyrimidinone (1a).** To a solution of di-*tert*-butyltricarboxylate (5.77 g, 22 mmol) in dry dichloromethane (25 mL) was added a solution of 6-aminohexanol (2.34 g, 20 mmol) in dry dichloromethane (40 mL) at room temperature under argon atmosphere. The reaction mixture showed immediate gas evolution ( $\text{CO}_2$ ) indicating the formation of the isocyanate.<sup>40</sup> Stirring was continued for 1 h. This reaction mixture was slowly added to a solution of 6-tridecylisocytosine in dry DMF at 90 °C under argon atmosphere. The reaction mixture was stirred for 4 h, after which it was cooled in an ice bath. The precipitate, which was formed, was filtered off, washed with hexane, and recrystallized from EtOH affording 5.05 g (52%) of crude product. A sample was purified using column chromatography (90 g  $\text{SiO}_2$ ,  $\text{CH}_2\text{Cl}_2/\text{MeOH}$  93/7,  $R_f = 0.3$ ) and subsequently recrystallized from MeOH to yield pure product. Mp 108.5 °C.  $^1\text{H}$  NMR (400 MHz,  $\text{CDCl}_3$ ):  $\delta$  0.90 (t, 3H,  $\text{CH}_2\text{CH}_3$ ), 1.2–1.8 (br m, 30H), 2.28 (t, 1H, OH), 2.48 (t, 2H, C(6) $\text{CH}_2$ ), 3.30 (q, 2H,  $\text{NHCH}_2$ ), 3.66 (q, 2H,  $\text{CH}_2\text{OH}$ ), 5.88 (s, 1H, C(5)H), 10.14 (t, 1H,  $\text{NHCH}_2$ ), 11.90 (s, 1H, C(2)NH), 13.23 (s, 1H, N(1)H).

**2-(4-(1-Pyrenyl)-1-oxo-butyl)oxyhexylureido-6-tridecyl-4[1H]-pyrimidinone (1b).** To a solution of 2, 4-(1-pyrenyl)butyric acid (68.4

mg, 0.24 mmol), and DMAP (10 mg, 0.02 mmol) in dry dichloromethane (10 mL) at 0 °C under an argon atmosphere was slowly added diisopropylcarbodiimide (36.7 mg, 0.29 mmol). The solution was allowed to slowly warm to room temperature and stirred for 25 h. The crude reaction mixture was concentrated in vacuo. The product was purified by column chromatography ( $\text{SiO}_2$ , gradient  $\text{CH}_2\text{Cl}_2/\text{MeOH}$  99.5/0.5  $\rightarrow$  95/5,  $R_f$  (95/5) = 0.38) and recrystallization from ethyl acetate, yielding 80 mg (49%) of pure **1b** as a fine white powder. Mp 105.5 °C  $^1\text{H}$  NMR (400 MHz,  $\text{CDCl}_3$ ):  $\delta$  0.89 (t, 3H,  $\text{CH}_2\text{CH}_3$ ), 1.26–1.67 (br m, 30H), 2.20 (m, 2H,  $\text{CH}_2\text{CH}_2\text{Pyrene}$ ), 2.36 (t, 2H,  $\text{CH}_2\text{-Pyrene}$ ), 2.47 (t, 2H, C(6) $\text{CH}_2$ ), 3.26 (q, 2H,  $\text{NHCH}_2$ ), 3.39 (t, 2H,  $\text{CH}_2\text{OC(O)}$ ), 4.14 (t, 2H,  $\text{OC(O)CH}_2$ ), 5.76 (s, 1H, C(5)H), 7.28–8.31 (br m, 9H, Pyrene), 10.19 (t, 1H,  $\text{CH}_2\text{NH}$ ), 11.73 (s, 1H, C(2)NH), 13.06 (s, 1H, N(1)H). Anal. Calcd for  $\text{C}_{44}\text{H}_{58}\text{N}_4\text{O}_4$ : C 74.75, H 8.27, N 7.92. Found: C 75.0, H 8.5, N 7.9.

**2-(2,6-Diisopropylphenylureido)-5,6-dimethyl-4[1H]-pyrimidinone (1e).** To a solution of di-*tert*-butylidicarbonate (0.88 g, 4.0 mmol) in DMSO (3 mL) was added DMAP (60 mg) and 2,6-diisopropylaniline (0.70 g, 3.9 mmol). The solution immediately showed gas evolution ( $\text{CO}_2$ ) indicating the formation of an isocyanate.<sup>41</sup> The mixture was slowly heated to 70 °C in 15 min under argon atmosphere. A sonicated dispersion of 5,6-dimethylisocytosine (0.50 g, 3.6 mmol) in DMSO was added and the solution was stirred for 21 h at 70 °C. The reaction mixture was then added to 75 mL of  $\text{CHCl}_3$  and extracted with water (3  $\times$  50 mL). The organic phase was dried over  $\text{MgSO}_4$  and reduced in vacuo. The remaining solids were then recrystallized from acetic acid to afford 390 mg (32%) of **1e** as a fine white microcrystalline powder, mp > 340 °C (degradation).  $^1\text{H}$  NMR (400 MHz,  $\text{CDCl}_3$ ):  $\delta$  1.20 (d, 6H,  $\text{CH}(\text{CH}_3)$ ), 1.25 (d, 6H,  $\text{CH}(\text{CH}_3)$ ), 1.87 (s, 3H, C(5) $\text{CH}_3$ ), 2.17 (s, 3H, C(6) $\text{CH}_3$ ), 3.19 (m, 2H,  $\text{CH}(\text{CH}_3)$ ), 7.20 (d, 2H, m-Ph), 7.30 (t, 1H, p-Ph), 11.76 (s, 1H,  $\text{NHPh}$ ), 12.56 (s, 1H,  $\text{NHC(O)NHPh}$ ), 12.94 (s, 1H, N(1)H).  $^{13}\text{C}$  NMR (100 MHz,  $\text{CDCl}_3$ ):  $\delta$  10.6 (C(5)- $\text{CH}_3$ ), 17.1 (C(6) $\text{CH}_3$ ), 23.1 ( $\text{CH}(\text{CH}_3)_2$ ), 24.2 ( $\text{CH}(\text{CH}_3)_2$ ), 28.6 ( $\text{CH}(\text{CH}_3)_2$ ), 114.0 (C(5)), 123.3 (p-Ph), 128.0 (m-Ph), 131.1 (C(6)), 142.6 (ipso-Ph), 146.6 (o-Ph), 153.2 (C(2)), 156.3 ( $\text{NHC(O)NH}$ ), 172.4 (C(4)). Anal. Calcd for  $\text{C}_{19}\text{H}_{26}\text{N}_4\text{O}_2$ : C 66.64, H 7.65, N 16.36. Found: C 66.4, H 7.8, N 16.4.

## Results

**Fluorescence.** Fluorescence spectroscopy enables the detection of strongly fluorescent species at extremely low concentrations. Model compound system **1b** was devised which, aside from the 2-ureido-4[1H]-pyrimidinone moiety, also contains a fluorescent pyrene group and a spacer of sufficient length to form pyrene excimers within the dimer.

To ascertain that, in the concentration range of interest ( $10^{-9}$ – $10^{-5}$  M), excimer fluorescence only occurs within dimers, fluorescence was measured at a concentration of  $10^{-5}$  M in the presence of a 1000-fold excess of *n*-butyl-1-ureido-4[1H]-pyrimidinone (**1c**) in chloroform. This reduces the concentration of **1b**•**1b** dimers to a negligible amount, preventing intra-dimer excimer formation. In this case no excimer emission was observed, while the monomer emission increased with respect to a pure  $10^{-5}$  M solution of pure **1b**.

For determination of the  $K_{\text{dim}}$  of **1b**, fluorescence spectra were measured in the concentration range from  $10^{-9}$  to  $10^{-6}$  M in chloroform, in toluene, and in chloroform saturated with water. The excimer band ( $\lambda_{\text{max}} = 478$  nm) was integrated from 500 to 600 nm, to exclude as much of the monomer emission bands ( $\lambda_{\text{max}} = 372$ – $399$  nm) as possible. The resulting integrated fluorescence emission intensities, normalized for concentration, are depicted in Figure 1.

From these data,  $K_{\text{dim}}$  was determined to be  $(5.7 \pm 0.6) \times 10^7 \text{ M}^{-1}$  ( $r^2 = 0.992$ ) for chloroform,  $(1.0 \pm 0.1) \times 10^7 \text{ M}^{-1}$  ( $r^2 = 0.995$ ) for wet chloroform, and  $(5.9 \pm 0.7) \times 10^8 \text{ M}^{-1}$

(39) Versteegen, R. M.; Sijbesma, R. P.; Meijer, E. W. *Angew. Chem., Int. Ed. Engl.* **1999**, *38*, 2917–2918.

(40) Peerlings, H. W. I.; Meijer, E. W. *Tetrahedron Lett.* **1999**, *40*, 1021–1024.

(41) Knolker, H.-J.; Braxmeier, T.; Schlechtingen, G. *Angew. Chem., Int. Ed. Engl.* **1995**, *34*, 2497–2499.

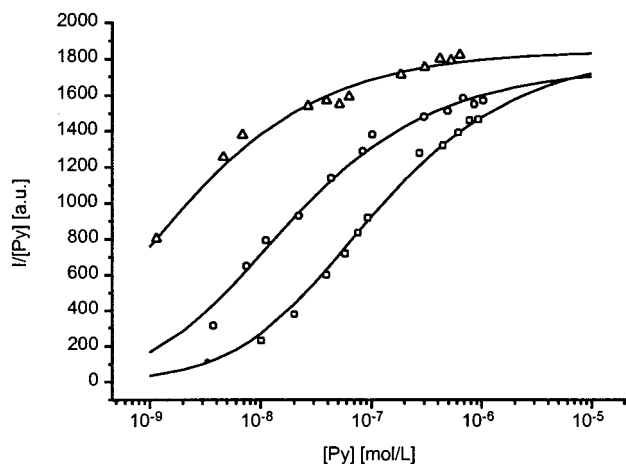


**Figure 1.** Plot of the normalized excimer fluorescence of **1b** vs concentration, measured in chloroform (○), chloroform saturated with water (□), and toluene (△), curves are derived from the nonlinear curve fit.

**Table 1.** Kinetic and Thermodynamic Parameters for Dimerization of **1** Determined at Different Temperatures with Errors Estimated from the Relevant Fitting Errors

	$k_d$ [ $s^{-1}$ ] (300 K) <sup>a</sup>	$E_{a,d}$ [kJ/mol] <sup>a</sup>	$K_{dim}$ [ $M^{-1}$ ] (298 K) <sup>b</sup>	$\Delta G^\circ_{dim}$ [kJ/mol] <sup>b</sup>
$CDCl_3$	$8.5 \pm 2$	$70 \pm 2$	$(5.7 \pm 0.6) \times 10^7$	-44
$CDCl_3 + H_2O$	$13 \pm 3$		$(1.0 \pm 0.1) \times 10^7$	-40
toluene- $d_8$	$0.6 \pm 0.3$	$62 \pm 15$	$(5.9 \pm 0.7) \times 10^8$	-50

<sup>a</sup> Exchange NMR. <sup>b</sup> Fluorescence spectroscopy in the nondeuterated analog.

( $r^2 = 0.993$ ) for toluene. This was done by nonlinear curve fits of the theoretical expression for the dimer concentration to the data. We assumed that, in this concentration range, the excimer

fluorescence intensity is linearly dependent on the dimer concentration (Table 1).

**Nuclear Magnetic Resonance.** Dynamic NMR and particularly magnetization transfer experiments are well suited for the study of dynamic processes in the frequency domain of  $1-10 s^{-1}$ . We have used both 2D exchange spectroscopy (EXSY<sup>31,32</sup>) and 1D double pulsed field gradient selective excitation (DPFGSE<sup>37,38</sup>) exchange experiments to study the chemical exchange of the 2-ureido-4[1H]-pyrimidinone dimers.

A prerequisite for the use of dynamic NMR is that the exchanging species are magnetically nonequivalent, so that the reactant and product of the exchange can be observed and integrated separately in the NMR spectrum. Exchange of 2-ureido-4[1H]-pyrimidinone dimers was studied using a combination of two differently substituted 2-ureido-4[1H]-pyrimidinones, which form a statistical mixture of two homodimers and a heterodimer. To maximize the chemical shift difference between the different dimers, phenyl-substituted derivatives **1d** and **1e** (Figure 2) were used. The phenyl group of **1e** can be in-plane with the pyrimidinone ring and induces a downfield shift of the signals of the 2-ureido-4[1H]-pyrimidinone bound to it, while the diisopropylphenyl group of **1e**, which is forced to be perpendicular to the pyrimidinone ring due to steric hindrance, induces an upfield shift of the signals of the opposing 2-ureido-4[1H]-pyrimidinone.

When **1d** and **1e** were mixed in a 1:1 ratio in  $CDCl_3$ , three dimeric species were observed in a 1:1:2 ratio of two homodimers and a heterodimer. The integrals of the 2-ureido-4[1H]-pyrimidinone molecules in the mixture show a 1:1 ratio for both dimeric forms as shown in Figure 2. The methyl group of **1d** shows a  $\Delta\delta$  of 0.17 ppm and the alkylidene proton of **1e**

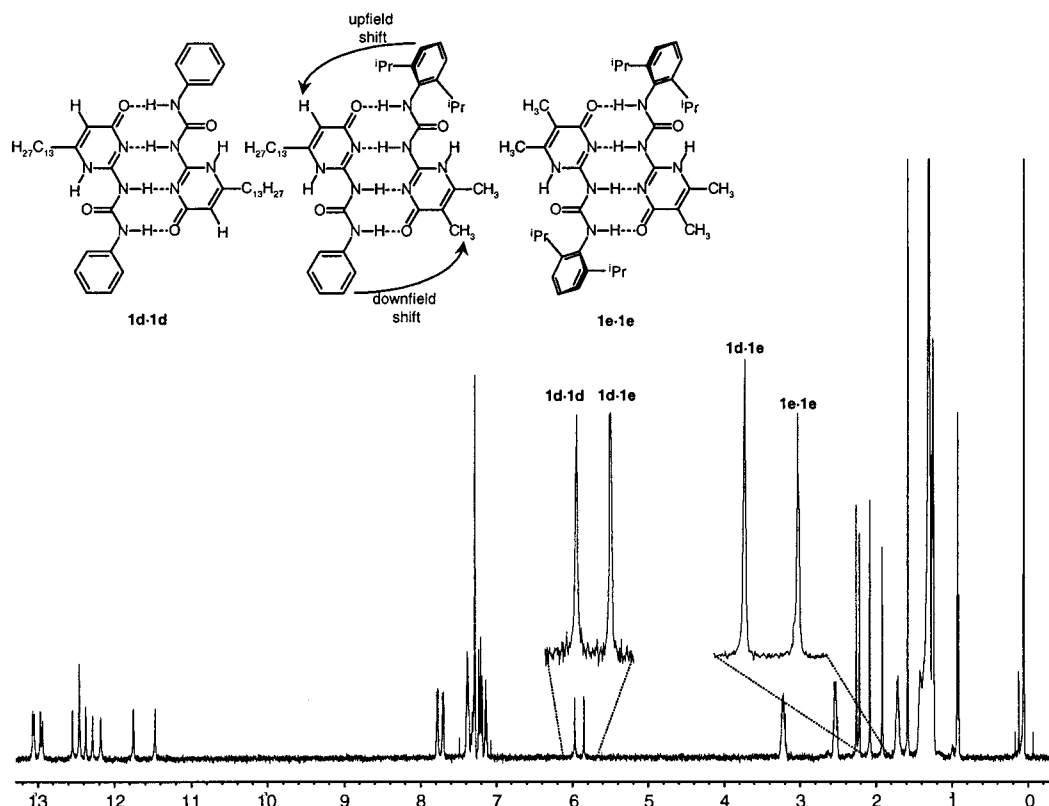


**Figure 2.** 1D  $^1H$  NMR spectrum of a 1:1 mixture of **1d** and **1e** in  $CDCl_3$ , containing the homo- and heterodimers shown above. Insets show splitting of homo- and heterodimer peaks at 5.9 ppm for the alkylidene proton and at 2.0 ppm for the methyl group.

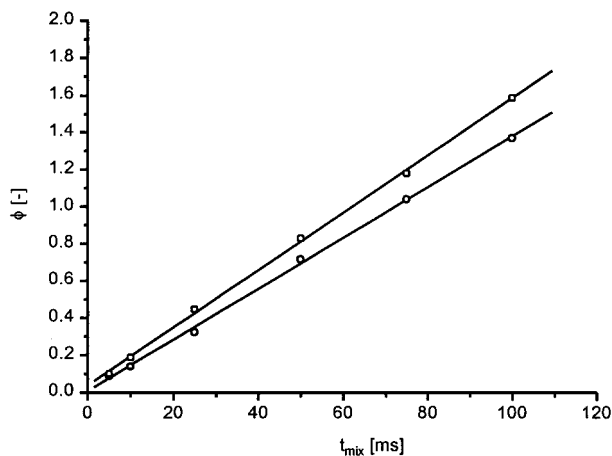


**Figure 3.** Plot of the transfer function  $\phi$  vs mixing time for equimolar mixtures of **1b** and **1c** at total concentrations of 10 (O) and 50 mM ( $\square$ ) (303 K in  $\text{CDCl}_3$ ).

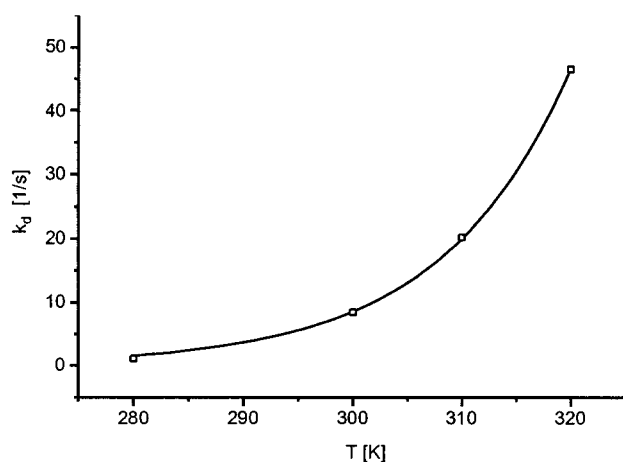


**Figure 4.** Dissociation rate constant plotted as a function of temperature for a 1:1 mixture of **1b** and **1c** in  $\text{CDCl}_3$  as determined with EXSY measurements. The data were fitted according to an Arrhenius equation using a linear least-squares fitting protocol on  $\ln(k_d)$ .

shows a  $\Delta\delta$  of 0.12 ppm between the homo- and heterodimer peaks, which is sufficient to integrate both peaks reliably at 400 MHz.

Several pathways for chemical exchange between homo- and heterodimers of **1d** and **1e** can be envisioned, including the following: (a) dissociation to monomers followed by random recombination or (b) association of two dimers, followed by interchange. To discriminate between these possibilities, a number of EXSY measurements at 10 and 50 mM in deuterated chloroform (303 K) were performed. The measurements were evaluated according to literature procedures,<sup>30,31</sup> using a linear curve fit of the transfer function  $\phi = k_{\text{ex}}t_{\text{mix}}$ , where  $k_{\text{ex}}$  is the exchange rate constant and  $t_{\text{mix}}$  is the mixing time (see Figure 3).

The exchange rate constants, in this case of equal populations, are equal to the total dissociation rate constants. The dissociation rate constants found for 10 and 50 mM solutions at 303 K in chloroform were nearly identical (14 ( $r^2 = 0.999$ ) and 15  $\text{s}^{-1}$  ( $r^2 = 0.999$ ), respectively), excluding an associative exchange mechanism, which would give concentration-dependent  $k_{\text{ex}}$  values. The fact that  $\phi$  is linear with  $t_m$  in these experiments, even at very short mixing times, shows that there is no long-lived intermediate and that only one mixing time can be used in subsequent experiments. A long-lived intermediate would

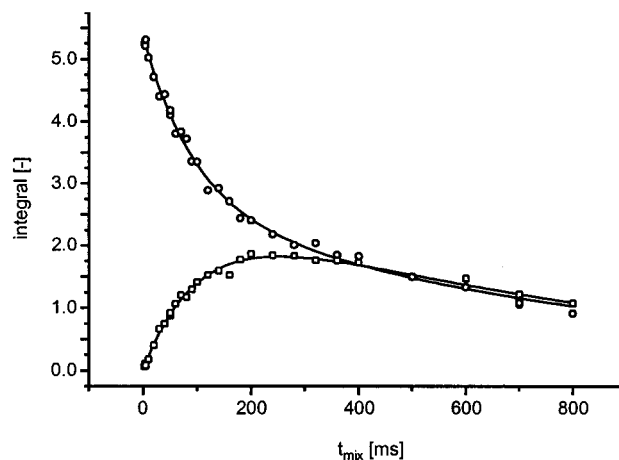


**Figure 5.** Integral of the methyl peaks of **1e** vs mixing time in a DPGSE experiment on a mixture of **1d** and **1e** in  $\text{CDCl}_3$  at 300 K, both the refocused peak (O, homodimer) and the dispersed peak ( $\square$ , heterodimer) are depicted.

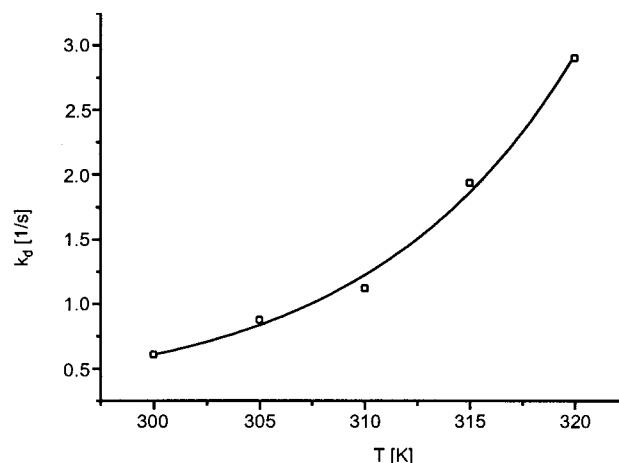


**Figure 6.** Dissociation rate constant plotted as a function of temperature for a mixture of **1d** and **1e** in toluene- $d_8$  as determined with DPGSE measurements. The data were fitted according to the Arrhenius equation using a linear least-squares fitting protocol on  $\ln(k_d)$ .

cause the exchange curve to approach a tangent of zero at low mixing times.

Temperature-dependent experiments were performed using a single mixing time of 50 ms at a concentration of 10 mM in  $\text{CDCl}_3$ . A plot of the dissociation rate constant vs temperature is shown in Figure 4. The dissociation rate constant is strongly temperature dependent, increasing 5-fold between 300 and 320 K. Fitting the Arrhenius equation to the data in Figure 4 results in a value of  $70 \pm 2$  kJ/mol ( $r^2 = 0.999$ ) for the activation energy of dissociation in chloroform. The dissociation rate constant at 300 K in  $\text{CDCl}_3$  is approximately 8.5  $\text{s}^{-1}$  (Table 1). This corresponds to hydrogen-bonded dimers with a preexchange lifetime of approximately 120 ms.

We have used a faster and simpler one-dimensional NOE technique, double pulsed field gradient selective excitation (DPFGSE),<sup>37,38</sup> to gather additional data on the exchange process. This technique allows us to use many different mixing times very quickly and, by avoiding conclusions based on just one measurement, get information that is more reliable. With the 2D technique it is not practical, simply because of time constraints, to measure a large range of mixing times. Relying on a few or even one measurement with one mixing time can lead to erroneous conclusions. The 1D DPGSE technique, because it is so fast, avoids this problem. The data, depicted in

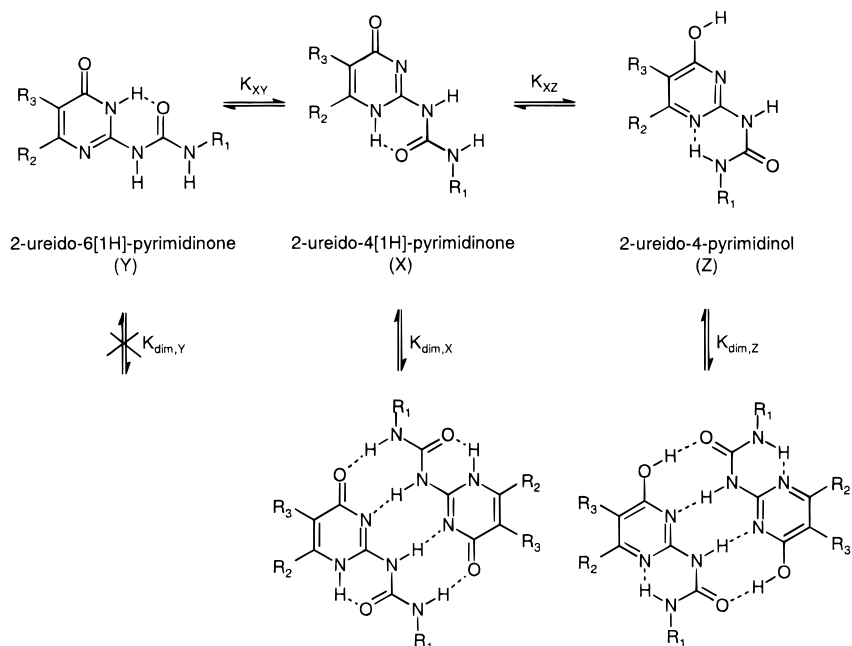


**Figure 7.** Tautomeric and association equilibria of **1** in solution.

Figure 5, were evaluated according to literature procedures.<sup>33</sup> The value found for the dissociation rate constant, based on selective inversion of both homo- and heterodimer peaks in chloroform (300 K), is  $8.8 \text{ s}^{-1}$  ( $r^2 = 0.99$ ). This is in good agreement with the value found with the EXSY measurement presented above ( $8.5 \text{ s}^{-1}$ ).

The DPGSE technique was used to investigate the stability of the hydrogen-bonded dimers in solvent systems with different polarities. It was particularly interesting to determine the stability of hydrogen-bonded dimers in an environment where water is present. The value found for the dissociation rate constant of a sample dissolved in deuteriochloroform saturated with water (55 mM) was  $13 \text{ s}^{-1}$  (300 K, 10 mM,  $r^2 = 0.99$ ), which is just 50% higher than the values found in dry chloroform (Table 1).

In octadeuteriotoluene, the dissociation rate constant is expected to be lower than that in  $\text{CDCl}_3$ , because of the lower polarity of toluene, making dimerization more favorable. A number of DPGSE experiments, in this solvent, were performed at temperatures between 300 and 320 K. The results are depicted in Figure 6. The dissociation rate constant at 300 K found in toluene is approximately  $0.6 \text{ s}^{-1}$ , almost 15 times lower than that in chloroform (Table 1). The activation energy for dissociation found in toluene is  $62 \pm 15 \text{ kJ/mol}$  ( $r^2 = 0.99$ ). It is evident, from the error found for this activation energy, that, due to the long mixing times required, determination of the rate constants becomes less accurate. Because of the long lifetimes of the exchanging species, the predominant process becomes  $T_1$  relaxation, not exchange. It is no longer possible to determine accurate thermodynamic parameters from these data.

## Discussion and Conclusions

The dimerization constant of **1** was previously estimated as exceeding  $2.2 \times 10^6 \text{ M}^{-1}$  (293 K in chloroform)<sup>15</sup> and Zimmerman<sup>22</sup> has shown that quadruply hydrogen bonded DDAA dimers of **2** have a dimerization constant of at least  $3 \times 10^7 \text{ M}^{-1}$  ( $\text{CDCl}_3$ ). Using fluorescence spectroscopy, we have now shown that the actual  $K_{\text{dim}}$  of **1** is significantly higher than previous estimates.

The  $K_{\text{dim}}$  value found in toluene is a factor of 10 higher than that found in chloroform, which is to be expected since toluene is more apolar than chloroform. In contrast, the value found in chloroform saturated with water is only a factor of 5 lower than that in dry chloroform. The water can hydrogen bond to the free monomer and will therefore compete with the association process, although this effect is much smaller than expected.

It was shown by Hammes<sup>42</sup> that, for strong triple hydrogen bonds in organic solvents, the association rate constant  $k_a$  is a diffusion-controlled parameter. If the same is assumed for the quadruply hydrogen bonded species described here, an estimate of the association rate constant, based on the viscosity of the solvent,<sup>43</sup> can be made, using the Stokes–Einstein and Debye equations.<sup>44</sup> The estimated diffusion-controlled association rate constants are  $6 \times 10^9$  and  $7.5 \times 10^9 \text{ M}^{-1} \text{ s}^{-1}$  (298 K) for chloroform and toluene, respectively.

The actual association rate constant  $k_a$  (at 298 K) in chloroform is estimated at  $5.0 \times 10^8 \text{ M}^{-1} \text{ s}^{-1}$  from the  $K_{\text{dim}}$  value ( $5.7 \times 10^7 \text{ M}^{-1}$ ) determined with fluorescence spectroscopy and from the  $k_d$  value determined with NMR ( $8.8 \text{ s}^{-1}$ ), assuming that the kinetic parameters are comparable for compounds **1b**, **1d**, and **1e**. The corresponding  $k_a$  value for toluene is  $3.5 \times 10^8 \text{ M}^{-1} \text{ s}^{-1}$ . These values are significantly lower than the theoretical diffusion-controlled association rate constants. As a result, it is concluded that association of **1**, in contrast to the triple hydrogen bonded systems studied by Hammes, is not diffusion controlled.

We have shown previously that monomeric as well as dimeric **1** exists as a mixture of tautomers (Figure 7). Although the predominant tautomer of monomeric **1** in  $\text{CDCl}_3$  solution is not known, tautomer Y, a tautomeric form which cannot dimerize via 4 hydrogen bonds, is the only tautomer observed in the mixed solvent system  $\text{CDCl}_3/\text{DMSO}$ .<sup>14</sup> We propose that this is

(42) Hammes, G. G.; Park, A. C. *J. Am. Chem. Soc.* **1968**, *90*, 4151–4157.

(43) Weast, R. C. *Handbook of Chemistry and Physics*, 64 ed.; Chemical Rubber Company Press: Boca Raton, FL, 1983.

(44) Amdur, I.; Hammes, G. G. *Chemical Kinetics: Principles and Selected Topics*; McGraw-Hill Book Co.: New York, 1963.

also the predominant tautomeric form of monomeric **1** in  $\text{CDCl}_3$  and toluene and that, as a result, the observed  $k_a$  is lower than the diffusion-controlled value. The unfavorable tautomeric equilibrium  $K_{XY}$  has the effect of reducing the fraction of molecular collisions that result in dimerization.

If the tautomeric equilibria would be completely on the side of the 4[1H]-pyrimidinone tautomer, the association rate constant is expected to be equal to the diffusion-limited association rate constant. This leads to a  $K_{\text{dim}}$  value, in the absence of tautomerization, of  $7 \times 10^8 \text{ M}^{-1}$  in chloroform and of  $10^{10} \text{ M}^{-1}$  in toluene (300 K).

We have shown that the 2-ureido-1[4H]-pyrimidinone moiety, which is synthetically easily accessible, exhibits a high equilibrium dimerization constant in common organic solvents. This makes it a very attractive molecule for the construction of

(45) Gonzalez, J. J.; Prados, P.; de Mendoza, J. *Angew. Chem., Int. Ed. Engl.* **1999**, *38*, 525–528.

(46) Beijer, F. H.; Sijbesma, R. P.; Vekemans, J. A. J. M.; Meijer, E. W.; Kooijman, H.; Spek, A. L. *J. Org. Chem.* **1996**, *61*, 6371–6380.

(47) Beijer, F. H.; Kooijman, H.; Spek, A. L.; Sijbesma, R. P.; Meijer, E. W. *Angew. Chem., Int. Ed. Engl.* **1998**, *37*, 75–78.

(48) Folmer, B. J. B.; Cavini, E.; Sijbesma, R. P.; Meijer, E. W. *Chem. Commun.* **1998**, 1847–1848.

supramolecular architectures in solution; some examples have already been shown.<sup>14–16,21,45–48</sup> A summary of all kinetic and thermodynamic parameters presented in this paper is shown in Table 1.

In the future we will apply the measurement techniques presented above to bifunctional 2-ureido-4[1H]-pyrimidinone derivatives to investigate the dynamics in polymeric systems directly.

**Acknowledgment.** Part of this investigation was supported by The Netherlands Foundation for Chemical Sciences (CW), with financial support from The Netherlands Organization for Scientific Research (NWO). We thank the Dutch National HF-NMR Facility in Nijmegen (The Netherlands), supported by CW, for time on the Bruker AVANCE DRX 600 spectrometer and in particular Jos Joordens for his help with the exchange NMR measurements. We also thank Michel Pepers for the initial work on EXSY NMR. Stefan Meskers is gratefully acknowledged for his help with the measurement and evaluation of the fluorescence spectra. We also thank Brigitte Folmer for her help with the synthesis of the model compounds

JA000435M